1. Rafał KOPACZ[1], 2. Michał HARASIMCZUK[1], 3. Radosław SOBIESKI[2], 4. Jacek RĄBKOWSKI[1]

Warsaw University of Technology (1), MARKEL Sp. z o.o. (2).
ORCID: 1. 0000-0002-2054-9821; 2. 0000-0002-5845-908X; 4. 0000-0001-8857-3505.

doi:10.15199/48.2023.05.35

Three-Level Interleaved Non-isolated DC/DC Converter as a Battery Interface in an EV Charging System with Bipolar DC-Link

Abstract. *This study presents a three-level, interleaved, non-isolated DC/DC converter designed as a battery interface for an EV fast-charging system with a bipolar +/- 750 V DC-link. A 20 kW prototype is exhibited based on a universal All-SiC MOSFET submodule for each leg. The core of the paper is the design of the experimental model, along with the description of the system's control, as well as validation in simulation and in introductory experiments. It is shown that such a converter employing modularized power modules can properly operate as the DC/DC interface.*

Streszczenie. *Niniejsze studium przedstawia trójpoziomowy, dwugałęziowy, nieizolowany przekształtnik DC/DC, zaprojektowany jako interfejs akumulatora dla systemu szybkiego ładowania pojazdów elektrycznych z dwubiegunowym obwodem prądu stałego +/- 750 V DC. Zaprezentowano prototyp o mocy 20 kW w oparciu o uniwersalny submoduł (All-SiC MOSFET) dla każdej gałęzi. Istotą pracy jest zaprojektowany model eksperymentalny wraz z opisem systemu sterowania, a także walidacja w symulacjach i początkowych eksperymentach. W artykule przedstawiono, że przekształtnik wykorzystujący zmodularyzowane moduły mocy może prawidłowo pracować jako interfejs prądu stałego.* ***(Trójpoziomowy, dwugałęziowy, nieizolowany przekształtnik prądu stałego jako interfejs baterii akumulatorów w systemie ładowania pojazdów elektrycznych z dwubiegunowym obwodem pośredniczącym prądu stałego)***.

Keywords: power electronics, DC/DC power conversion, multilevel converters, electric vehicle charging systems.
Słowa kluczowe: energoelektronika, przekształcanie energii prądu stałego, przekształtniki wielopoziomowe, systemy ładowania pojazdów elektrycznych.

Introduction

The expansion of electric vehicles (EVs) is an ongoing trend in today's society, with the EV market growing at a very fast rate [1]. Therefore, to fully employ the potentially great number of EVs, proper charging infrastructure is a necessity [2]. This is especially crucial in terms of the ability to charge the EVs rapidly, e.g., on highways, where the utilization of highly-performant fast and ultra-fast charging stations is required.

There is a large variety of approaches that can be employed to construct fast charging stations that differ in the voltage levels, the presence of additional battery energy storage, as well as the grid structure (unipolar vs. bipolar) [3, 4]. Here, an EV charging system with a bipolar DC grid with +/- 750 V and extra battery energy storage is considered, as such a system is considered advantageous compared to more conventional approaches [5-7]. To be more specific, the bipolar structure allows for higher efficiency and flexibility, medium voltage (MV) level lowers the conduction power losses even further, especially for the more-and-more common 800 V loads, while the auxiliary battery provides to the possibility to operate in an off-grid situation in case of grid power shortage or to allow for grid support from the charging station.

When the battery interface converter required to connect the station's DC-link and the battery energy storage is considered, a number of topologies can be used [4, 8, 9]. However, in the mentioned bipolar charging system, several topologies are not appropriate by default due to a vast array of requirements. These necessities include bidirectional operation, low battery-side ripples, and high efficiency. Furthermore, the topology has to be capable of a 3-pole (+750 V/0 V/- 750 V) connection with the ability of DC bus voltage balancing. Here, based on the literature review, a three-level, two-phase, interleaved, non-isolated DC/DC converter with 1.2 kV SiC transistors was chosen, as wide-bandgap power devices are characterized by a vast number of advantages compared to Si-based transistors [10, 11]. The three-level topology provides the possibility to employ well-performing off-the-shelf 1.2 kV SiC MOSFETs and obtain lower power losses compared to other approaches [12], as well as the option to balance the DC grid [13] with low general complexity. Moreover, the interleaved two-phase topology shows good perspective in terms of low output ripples [10, 14, 15], especially important for cooperating with a battery energy storage. Finally, the chosen converter topology allows to include a universal All-SiC submodule [16] that can be used as the power electronics building block for each converter in the EV fast charging system, e.g., the presented DC/DC converter and the grid converter [17].

The paper is constructed as follows. After the succinct introduction, the second section describes the three-level interleaved DC/DC converter with its' operation principles, while the third section is focused on the simulation study. Then, the prototype with the initial experiments is described in the next section. Finally, the paper is concluded in the last section.

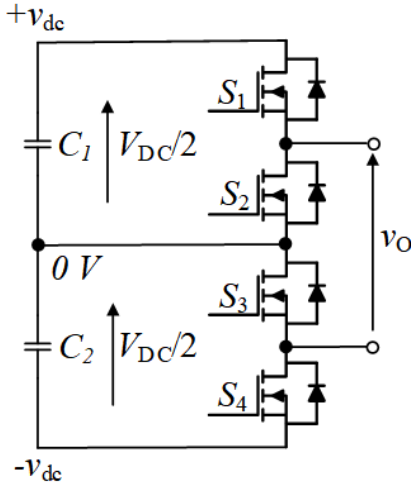

Fig.1. One leg of the three-level DC/DC converter.

Three-level interleaved DC/DC converter

The leg of the three-level DC/DC converter shown in Fig. 1 is basically two conventional two-level synchronous DC/DC converters connected in series. Therefore, the maximum transistor drain-source voltage V_{DS} is maximally $V_{DC}/2$ (omitting overshoots) and widely available 1200 V

SiC MOSFETs can be used when V_{DC} of 1500 V is considered. Moreover, since the system is multilevel, it is possible to shape the output voltage more flexibly. The basic converter switching states are depicted in Table 1 and Fig. 2. As can be seen, the output voltage of the leg can reach the full DC-link voltage V_{DC}, half of the V_{DC} voltage, or no voltage at all. Moreover, to control the converter, two control signals per leg (S_1=!S_2 and S_4=!S_3) are sufficient. Furthermore, the middle voltage states can be employed to decide on the voltage distribution between the two DC-link capacitors, which provides a voltage balancing possibility. Finally, the converter can operate bidirectionally, as long as the battery-side voltage is lower than the DC-bus-side voltage. However, for sake of simplicity, only buck mode is considered in this paper. All in all, the three-level DC/DC converter is a straightforward topology that has a low component count and is capable of reaching high efficiencies.

Table 1. Basic switching states of the DC/DC converter in buck mode

State	S_1	S_2	S_3	S_4	Output voltage
High state (H)	1	0	0	1	V_{DC}
Medium state 1 (M1)	1	0	1	0	$V_{DC}/2$
Medium state 2 (M2)	0	1	0	1	$V_{DC}/2$
Zero state (Z)	0	1	1	0	0

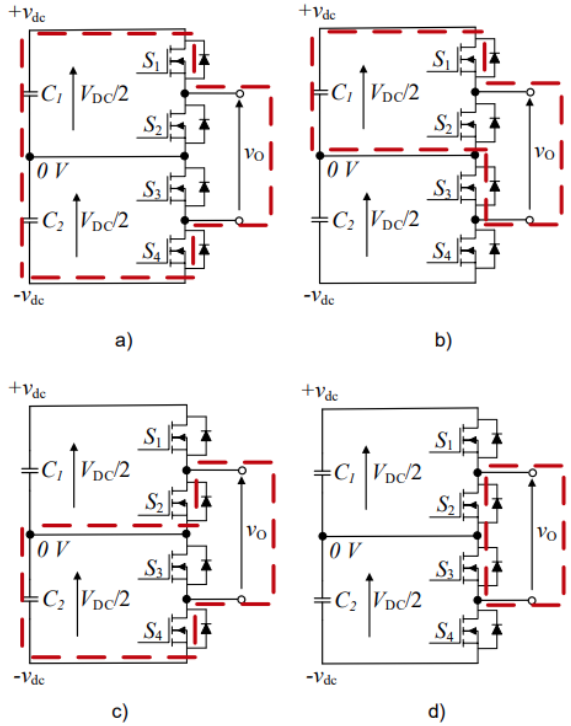

Fig. 2. Basic switching states of the DC/DC converter in buck mode: a) high state, b) medium state 1, c) medium state 2, d) zero state.

Using interleaved structure is a simple method to lower the output ripples of the converter, especially important for battery-oriented systems. Here, a two-phase system is considered, as for the considered battery system with 800 V nominal voltage, operating points near D=0.5 result in the lowest ripples. There are several ways to control the interleaved phases in the three-level converter, namely the classic, N-type, and Z-type interleaving methods [15]. For the considered converter, the N-type scheme shown in Fig. 3 was used, as it is characterized by lower output current ripples compared to the classic approach and lower EMI generation when put against the Z-type method.

The control diagram of the three-level DC/DC converter is presented in Fig. 4. Please note that even though the figure shows the system operating in buck mode for simplicity, this converter with the control system is also applicable in boost mode with the opposite direction of power flow, as long as the voltage controller is driven by the grid-side DC voltage values, depicted as V_{dc} in Fig. 4.

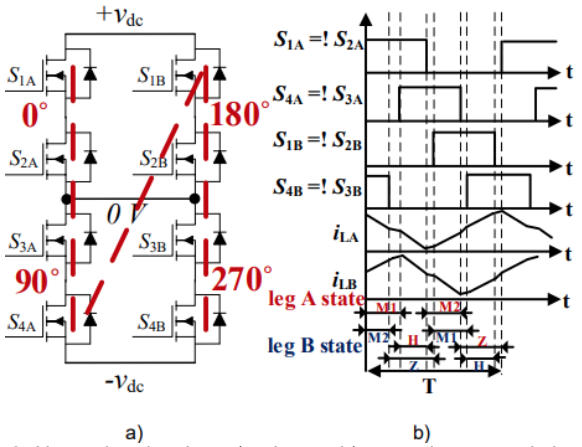

Fig.3. N-type interleaving: a) scheme, b) exemplary control signals, with inductor currents and switching states for each converter leg

In the system, the core control path consists of a primary current PI (proportional-integral) controller and a secondary voltage controller, where the reference value of the output voltage is given. Using the output of the main current control, the dominant part of duty cycles D_A (for leg A) and D_B (for leg B) are calculated and used to drive the converter.

However, additional balancing measures are required for the proper operation of the converter. Firstly, the 3-pole DC bus connection necessitates leveling the DC voltages at capacitors C_1 and C_2. Based on an error value from the difference between the measured v_{dc1} and v_{dc2} voltages, a voltage-balancing PI controller regulates the duty cycles of the converter. The output of the controller is either added (for signal S_4=!S_3) or subtracted (in the case of signal S_1=!S_2) to the duty cycle value. Therefore, such an approach allows for voltage balancing without affecting the output voltage.

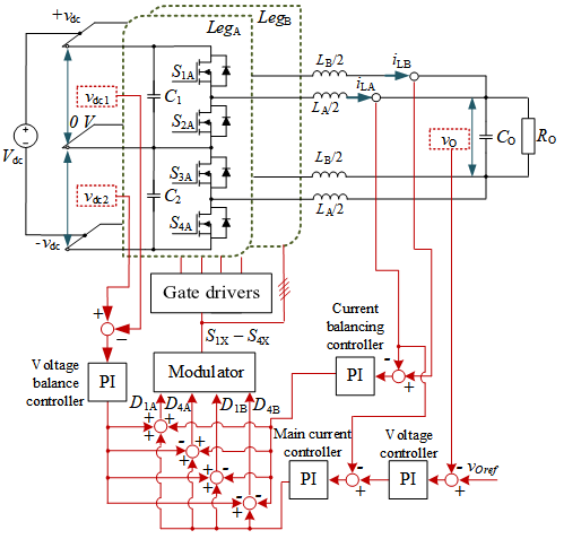

Fig.4.The DC/DC converter in buck mode with the control diagram.

Furthermore, balancing currents between the interleaved legs is also a necessity to limit the currents circulating in the inductors and minimize additional power losses [18]. This can be achieved through two separate control paths consisting of a voltage and a current controller for each leg. However, using this method, the total count of controllers is five. Thus, in the presented system, to limit the number of regulators, another approach was assumed. The core control path (voltage and main current controllers) is used to set the duty cycles for both legs, and an additional current controller using the difference between the inductor currents i_{LA} and i_{LB} as an error is used. Therefore, the output from the current balancing controller is added to D_A value and subtracted from D_B, and similarly, as in the voltage balancing controller, the output is unaffected. Moreover, apart from lowering the number of total regulators to four, the current balancing controller is less susceptible to noise, as the error uses two measured values as an input, and therefore the interferences cancel out.

Simulation study

At first, in order to preliminarily validate the three-level interleaved DC/DC converter, a simulation study in PLECS was performed. The schematic and control used in the simulations were prepared according to the description in the previous section and shown in Fig. 4. The parameters of the tests in the simulation study are depicted in Table 2.

Table 2. Parameters of the simulation and experimental study

Battery-side (output) voltage	800 V – simulation case 1 590 V – sim. case 2, experimental
DC bus-side voltage	1.5 kV DC – simulation case 1 800 V DC – sim. case 2, experimental
Switching frequency	50 kHz
Filter inductors	4 x 150 µH
Battery-side capacitor	60 µF
DC-link capacitors	4 x 60 µF
Power transistors	8 x NTH4L040N120SC1
Maximum tested output power	20 kW – simulation case 1 10 kW - sim. case 2, experimental

The results from the exemplary simulation performed in the steady-state are showcased in Fig. 5 and 6. The results from the study at nominal operating point at 1500 V input, 800 V output, and 20 kW power is depicted in Fig. 5, while another point, directly correlating with the exemplary experimental test shown further in the paper, performed at 800 V input, 590 V output, and power of 10 kW is shown in Fig. 6. As can be observed, the control system operates as assumed: the output voltage is steady at the reference value, the DC bus voltages are well-balanced with minimal ripples, and the inductor currents are levelled as well. Moreover, even though the momentary currents of individual inductors are high, due to the interleaved structure and N-type modulation, the ripple of the sum inductor current is at low levels, at roughly 5% of the nominal value. Therefore, ripples of both output current and voltage are minuscule. However, it is worth noting that in a real-life application, the connections, e.g., cables, to the battery energy storage system can be lengthy, and thus extra parasitic inductance appears, causing the output ripples to increase radically. Moreover, it can bee seen that using the N-type modulation, the current shape is either triangular (for duty near 0.5), or closer to a trapezoidal shape. All in all, the simulations prove that the DC/DC converter can adequately operate with the presented control system.

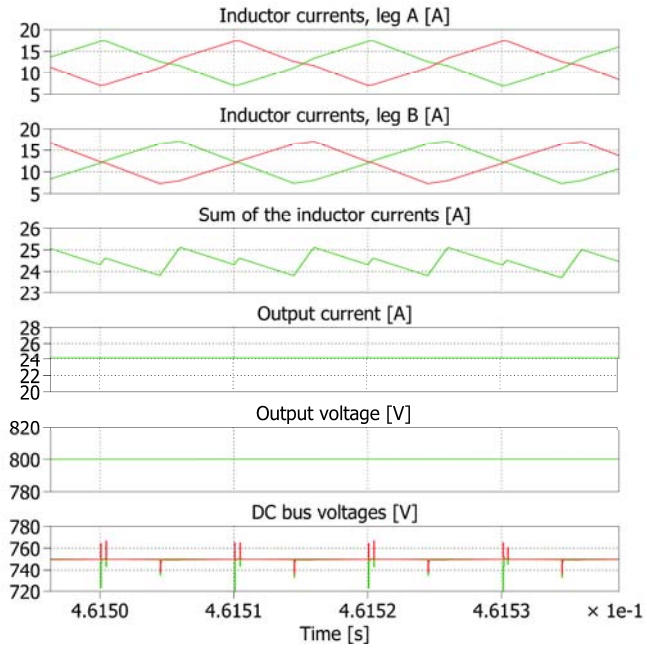

Fig.5. Simulation results of the DC/DC converter – case 1, 1500 V input, 800 V output, 20 kW power.

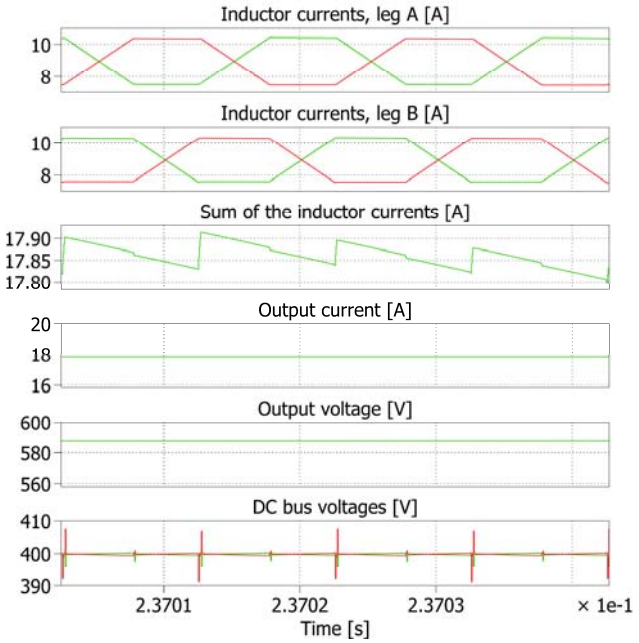

Fig.6. Simulation results of the DC/DC converter – case 2, 800 V input, 590 V output, 10 kW power.

Experimental study

The second step of the converter validation included the construction of the prototype and performing the initial experimental tests. To build the system, power modules described in [13], and depicted in Fig. 7, were used as the converter legs. Here, as the power devices, 1.2 kV SiC MOSFETs (NTH4L040N120SC1) were used, as they are characterized by low on-state resistance of 40 mΩ, as well as an external Kelvin source connection for improved switching performance. Apart from the four power transistors, the power modules contain two film capacitors (60 µF/800 V) and two gate driver modules built based on ICs from Texas Instruments (UCC21750), also providing protection measures for the power transistors. Finally, the power module also includes a PCB that connects all the

components and a highly-performant heatsink with forced air cooling (Fischer Elektronik LAM6).

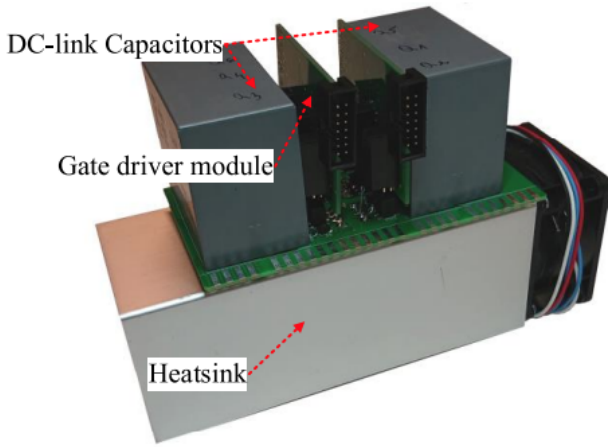

Fig.7. Experimental model of one leg of the DC/DC converter.

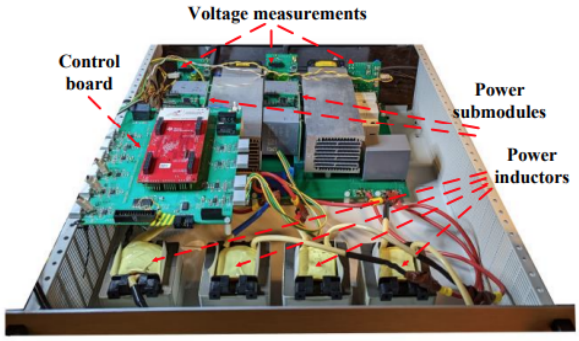

Fig.8. Prototype of the full three-level interleaved DC/DC converter

The full DC/DC converter contains two of the power modules. Moreover, the experimental model consists of four 150 µH inductors from Feryster (DEMS-65X54/0,15/37), an output capacitor (800 V/60 µF), a control board based on TMS320F28379D, and a number of measurement circuits. Except for the core ones enumerated in the second section (two DC bus voltage measurements, output voltage measurement, and two inductor current meters), there are more measurements required for the full EV charging station operation. To be more specific, it is required to measure the power flow into and out of the converter. Thus, additional output current meter and two input current measurements were added (one per half of the DC bus). All the current meters were constructed using LEM transducers, LA-55 for the inductor currents and LAH-50 for the DC currents. The voltage measurements were based on self-made PCBs, using optocouplers and amplifiers to construct an isolated voltmeter system. The whole converter fits in a 3U rack case. The photo of the full three-level interleaved converter is shown in Fig. 8.

A test setup, according to Fig. 4 was used for the experimental tests, employing Magna Power DC supply (800 V, 12.5 A) and a resistive load. The oscillograms were acquired using Tektronix MSO34 oscilloscope with isolated voltage probes (Tektronix THDP0100 and THDP0200) and current probes (Tektronix TCP303, TCP 202A, and TCP0030A).

The results from the initial experiments are presented in Fig. 9 showcase the proper operation of the DC/DC converter. The exemplary test was performed at 10 kW power, 800 V, and a load of 34 Ω, resulting in a voltage gain of roughly 0.74. Analyzing Fig. 9a, it can be seen that the DC-link voltages are well leveled using the presented voltage balancing method, with a difference below 1% of the nominal DC voltage (roughly 7 V) and some minor overshoots appearing at the time of transistor switchings (at approximately 40 V). Therefore, the voltage among the transistors in the multilevel structure is balanced as well, providing safe operating conditions for the converter. Furthermore, the output current of the converter is characterized by very low ripples – 0.6 A, corresponding to less than 4% of the i_O steady-state value. This is crucial since the converter is designed to cooperate with a battery energy storage system. Finally, the output voltage is stable and reaches the reference value of 590 V.

Fig. 9b is focused on exhibiting the performance of the inductors. As can be observed, thanks to the current balancing regulator, the inductor currents are equal in terms of the mean value for both legs, limiting the possible circulating current described in the previous sections. Moreover, even though the momentary current ripples of the individual inductors are on a significant level (with peak-to-peak currents at roughly 9.3 A compared to a maximum value of 12.5 A), by applying the N-type interleaving method, the sum inductor current flowing to the output capacitor is steady, with current ripples at approximately 8% of the nominal mean value (16.7 A).

All in all, it has been validated that the DC/DC converter prototype with the presented control method behaves as anticipated, with balanced DC-link voltages and inductor currents and low output ripples. Thus, it can be effectively applied in a bipolar grid-based EV charging station.

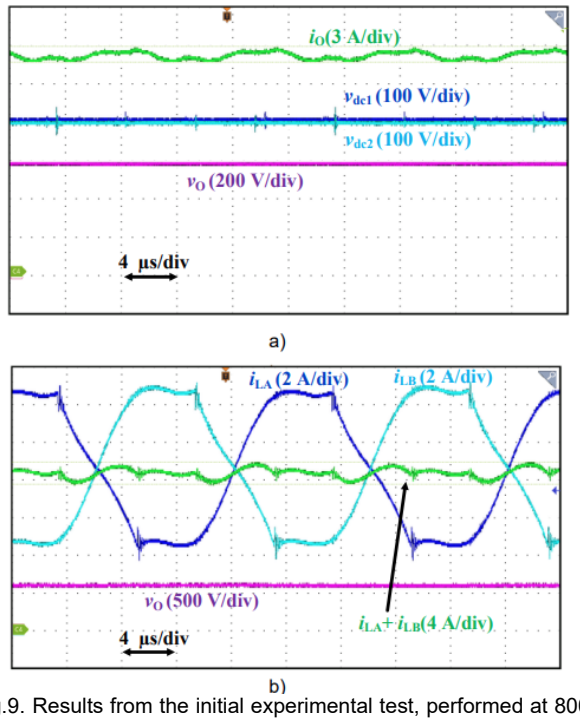

Fig.9. Results from the initial experimental test, performed at 800 V DC voltage, 10 kW power and a load of 34 Ω, voltage gain of roughly 0.74: a) general view with output current and voltage, as well as the DC bus-side voltages; b) inductors-focused view with i_{LA}, i_{BA}, and sum inductor current of the positive output pole $i_{LA} + i_{LAB}$

Conclusion

In this paper, a three-level, interleaved, non-isolated DC/DC converter, rated at 1.5 kV DC voltage, 20 kW power, and built using a modular structure with SiC MOSFETs, is presented. Based on an analysis of the converter, its control, and validation through simulation and initial experimental study, it is shown that the DC/DC converter can be effectively used as a battery interface for an EV fast-

charging system with a bipolar +/- 750 V DC-link, as it provides satisfactory performance, low output ripples, as well as balanced inductor currents and DC bus voltages for various operating points.

Further works will include a full experimental study at rated current/voltage levels is planned, both in boost and buck modes. Moreover, an analysis of different inductor configurations, including coupled structures, is also planned. Finally, experiments with the DC/DC converter operating in the full EV charging station are projected, including the cooperation with the grid converter, a battery energy storage system, as well as with other DC/DC converters destined for interfacing the EVs connected to the station.

The research leading to these results has received funding from the EEA/Norway Grants 2014–2021.

***Authors**: Rafał Kopacz, MSc., Warsaw University of Technology, Institute of Control and Industrial Electronics, Koszykowa 75, 00-662 Warsaw, E-mail: rafal.kopacz@pw.edu.pl; Michał Harasimczuk, Ph.D., Warsaw University of Technology, Institute of Control and Industrial Electronics, Koszykowa 75, 00-662 Warsaw, E-mail: michal.harasimczuk@pw.edu.pl; Radosław Sobieski, MSc.,* MARKEL Sp. z o.o.*, Okulickiego 7/9, 05-500 Piaseczno, E-mail: radek.sobieski@markel.pl; Jacek Rąbkowski, DSc. Ph.D., Warsaw University of Technology, Institute of Control and Industrial Electronics, Koszykowa 75, 00-662 Warsaw, E-mail: jacek.rabkowski@pw.edu.pl*

REFERENCES

[1] A. Ghosh, “Possibilities and Challenges for the Inclusion of the Electric Vehicle (EV) to Reduce the Carbon Footprint in the Transport Sector: A Review,” *Energies,* vol. 13, no. 10, 2020, doi: 10.3390/en13102602.

[2] A. Hussain, V.-H. Bui, J.-W. Baek, and H.-M. Kim, “Stationary Energy Storage System for Fast EV Charging Stations: Simultaneous Sizing of Battery and Converter,” *Energies,* vol. 12, no. 23, 2019, doi: 10.3390/en12234516.

[3] S. Rivera, R. L. F, S. Kouro, T. Dragičević, and B. Wu, “Bipolar DC Power Conversion: State-of-the-Art and Emerging Technologies,” *IEEE Journal of Emerging and Selected Topics in Power Electronics,* vol. 9, no. 2, pp. 1192-1204, 2021, doi: 10.1109/JESTPE.2020.2980994.

[4] M. A. H. Rafi and J. Bauman, “A Comprehensive Review of DC Fast-Charging Stations With Energy Storage: Architectures, Power Converters, and Analysis,” *IEEE Transactions on Transportation Electrification,* vol. 7, no. 2, pp. 345-368, 2021, doi: 10.1109/TTE.2020.3015743.

[5] S. Rivera and B. Wu, “Electric Vehicle Charging Station With an Energy Storage Stage for Split-DC Bus Voltage Balancing,” *IEEE Transactions on Power Electronics,* vol. 32, no. 3, pp. 2376-2386, 2017, doi: 10.1109/TPEL.2016.2568039.

[6] I. Aghabali, J. Bauman, P. J. Kollmeyer, Y. Wang, B. Bilgin, and A. Emadi, “800-V Electric Vehicle Powertrains: Review and Analysis of Benefits, Challenges, and Future Trends,” *IEEE Transactions on Transportation Electrification,* vol. 7, no. 3, pp. 927-948, 2021, doi: 10.1109/TTE.2020.3044938.

[7] Y. Tahir *et al.*, “A state-of-the-art review on topologies and control techniques of solid-state transformers for electric vehicle extreme fast charging,” *IET Power Electronics,* vol. 14, no. 9, pp. 1560-1576, 2021, doi: https://doi.org/10.1049/pel2.12141.

[8] Y. Du, X. Zhou, S. Bai, S. Lukic, and A. Huang, “Review of non-isolated bi-directional DC-DC converters for plug-in hybrid electric vehicle charge station application at municipal parking decks,” in *2010 Twenty-Fifth Annual IEEE Applied Power Electronics Conference and Exposition (APEC)*, 21-25 Feb. 2010 2010, pp. 1145-1151, doi: 10.1109/APEC.2010.5433359.

[9] P. Falkowski, M. Korzeniewski, A. Ruszczyk, and K. Kóska, "Analysis and design of high efficiency DC/DC buck converter," *Przegląd Elektrotechniczny,* vol. 5, pp. 150-156, 2016.

[10] P. Zimoch, "Interleaved quasi–resonant boost converter with Si and SiC devices," *Przegląd Elektrotechniczny,* vol. 7, pp. 183-188, 2018.

[11] P. Czyż, A. Reinke, and M. Michna, "Application of GaN transistors in high-frequency DC/DC converters," *Przegląd Elektrotechniczny,* vol. 1, pp. 333-339, 2017.

[12] S. Dusmez, A. Hasanzadeh, and A. Khaligh, “Loss analysis of non-isolated bidirectional DC/DC converters for hybrid energy storage system in EVs,” in *2014 IEEE 23rd International Symposium on Industrial Electronics (ISIE)*, 1-4 June 2014 2014, pp. 543-549, doi: 10.1109/ISIE.2014.6864671.

[13] L. Tan, B. Wu, V. Yaramasu, S. Rivera, and X. Guo, “Effective Voltage Balance Control for Bipolar-DC-Bus-Fed EV Charging Station With Three-Level DC–DC Fast Charger,” *IEEE Transactions on Industrial Electronics,* vol. 63, no. 7, pp. 4031-4041, 2016, doi: 10.1109/TIE.2016.2539248.

[14] V. Monteiro, J. C. Ferreira, A. A. N. Meléndez, C. Couto, and J. L. Afonso, “Experimental Validation of a Novel Architecture Based on a Dual-Stage Converter for Off-Board Fast Battery Chargers of Electric Vehicles,” *IEEE Transactions on Vehicular Technology,* vol. 67, no. 2, pp. 1000-1011, 2018, doi: 10.1109/TVT.2017.2755545.

[15] S. Lu, M. Mu, Y. Jiao, F. C. Lee, and Z. Zhao, “Coupled Inductors in Interleaved Multiphase Three-Level DC–DC Converter for High-Power Applications,” *IEEE Transactions on Power Electronics,* vol. 31, no. 1, pp. 120-134, 2016, doi: 10.1109/TPEL.2015.2398572.

[16] R. Kopacz, M. Harasimczuk, B. Lasek, R. Miśkiewicz, and J. Rąbkowski, "All-SiC ANPC Submodule for an Advanced 1.5 kV EV Charging System under Various Modulation Methods," *Energies,* vol. 14, no. 17, 2021, doi: 10.3390/en14175580.

[17] M. Harasimczuk, K. Kalinowski, R. Miskiewicz, R. Kopacz, B. Lasek, and J. Rabkowski, “Three-Level ANPC Converter as an Input Stage of an EV ChargingSystem with Bipolar DC Link,” in *PCIM Europe 2022; International Exhibition and Conference for Power Electronics, Intelligent Motion, Renewable Energy and Energy Management*, 10-12 May 2022, pp. 1-6, doi: 10.30420/565822256.

[18] L. Tan, N. Zhu, and B. Wu, “An Integrated Inductor for Eliminating Circulating Current of Parallel Three-Level DC–DC Converter-Based EV Fast Charger,” *IEEE Transactions on Industrial Electronics,* vol. 63, no. 3, pp. 1362-1371, 2016, doi: 10.1109/TIE.2015.2496904.